THE JOURNAL OF BIOLOGICAL CHEMISTRY VOL. 286, NO. 43, pp. 37458–37469, October 28, 2011

Overexpression of KLF15 Transcription Factor in Adipocytes of Mice Results in Down-regulation of SCD1 Protein Expression in Adipocytes and Consequent Enhancement of Glucose-induced Insulin Secretion*[S]

Received for publication, March 23, 2011, and in revised form, August 1, 2011 Published, JBC Papers in Press, August 23, 2011, DOI 10.1074/jbc.M111.242651

Tomoki Nagare,[a,b,c] Hiroshi Sakaue,[c,d1] Michihiro Matsumoto,[a,b1] Yongheng Cao,[a,b] Kenjiro Inagaki,[a,b] Mashito Sakai,[a,b] Yasuhiro Takashima,[c] Kyoko Nakamura,[c] Toshiyuki Mori,[c] Yuko Okada,[c] Yasushi Matsuki,[e] Eijiro Watanabe,[e] Kazutaka Ikeda,[f,g,h] Ryo Taguchi,[g,h,i] Naomi Kamimura,[j] Shigeo Ohta,[j] Ryuji Hiramatsu,[e] and Masato Kasuga,[b,c2]

From the [a]Department of Molecular Metabolic Regulation, [b]Diabetes Research Center, Research Institute, National Center for Global Health and Medicine, Tokyo 162-8655, the [c]Division of Diabetes, Metabolism, and Endocrinology, Department of Internal Medicine, Kobe University Graduate School of Medicine, Kobe 650-0017, the [d]Department of Nutrition and Metabolism, Institute of Health Biosciences, University of Tokushima Graduate School, Tokushima 770-8503, the [e]Pharmacology Research Laboratories, Dainippon Sumitomo Pharma Co. Limited, Takarazuka 665-0051, the [f]Institute for Advanced Biosciences, Keio University, Yamagata 997-0052, the [g]Department of Metabolome, Graduate School of Medicine, University of Tokyo, Tokyo 113-0033, the [h]Core Research for Evolutional Science and Technology Program, Japan Science and Technology Agency, Saitama 332-0012, the [i]Department of Biomedical Sciences, College of Life and Health Sciences, Chubu University, Aichi 487-8501, and the [j]Department of Biochemistry and Cell Biology, Institute of Development and Aging Sciences, Graduate School of Medicine, Nippon Medical School, Kawasaki 211-8533, Japan

Krüppel-like factor 15 (KLF15), a member of the Krüppel-like factor family of transcription factors, has been found to play diverse roles in adipocytes *in vitro*. However, little is known of the function of KLF15 in adipocytes *in vivo*. We have now found that the expression of KLF15 in adipose tissue is down-regulated in obese mice, and we therefore generated adipose tissue-specific KLF15 transgenic (aP2-KLF15 Tg) mice to investigate the possible contribution of KLF15 to various pathological conditions associated with obesity *in vivo*. The aP2-KLF15 Tg mice manifest insulin resistance and are resistant to the development of obesity induced by maintenance on a high fat diet. However, they also exhibit improved glucose tolerance as a result of enhanced insulin secretion. Furthermore, this enhancement of insulin secretion was shown to result from down-regulation of the expression of stearoyl-CoA desaturase 1 (SCD1) in white adipose tissue and a consequent reduced level of oxidative stress. This is supported by the findings that restoration of SCD1 expression in white adipose tissue of aP2-KLF15 Tg mice exhibited increased oxidative stress in white adipose tissue and reduced insulin secretion with hyperglycemia. Our data thus provide an example of cross-talk between white adipose tissue and pancreatic β cells mediated through modulation of oxidative stress.

Obesity is characterized by an increased amount of adipose tissue and is associated with various complications, including insulin resistance, type 2 diabetes, dyslipidemia, and atherosclerosis (1, 2). Mammals possess two types of adipose tissue, white adipose tissue (WAT)[3] and brown adipose tissue (BAT). White adipocytes play an important role in obesity by secreting numerous bioactive substances known as adipocytokines (or adipokines) as well as by storing energy in the form of triglyceride. Through the secretion of adipokines, white adipocytes affect other tissues, including the liver, skeletal muscle, β cells of the pancreas, and the central nervous system. Brown adipocytes, which contain abundant mitochondria, also play an important role in obesity by dissipating energy through adaptive thermogenesis. Both white and brown adipocytes thus influence systemic energy metabolism (3).

Krüppel-like factor 15 (KLF15), a member of the Krüppel-like factor family of transcription factors, was first identified as a molecule that binds to the promoter of the gene for CLC-K1, a kidney-specific CLC chloride channel (4). We and others subsequently showed that KLF15 regulates gene expression in various cell types, including adipocytes (5–7), myocytes (7, 8), and hepatocytes (9, 10). Characterization of mice lacking KLF15 implicated this protein in the regulation of gluconeogenesis with amino acids as substrates (11). However, little is known of the role of KLF15 in adipose tissue *in vivo*.

Stearoyl-CoA desaturase 1 (SCD1), a member of the fatty acid desaturase family, has recently been associated with obesity, diabetes, immune disorders, and inflammation (12, 13). Mice deficient in SCD1 either globally (14) or specifically in the

* This work was supported by a grant-in-aid for creative scientific research (to M. K. and M. M.), a grant-in-aid for scientific research (c) (to H. S. and M. M.) from the Ministry of Education, Culture, Sports, Science, and Technology of Japan, Grant from the National Center for Global Health and Medicine 21S116 (to M. M.), a grant from Takeda Science Foundation (to H. S. and M. M.), and a grant from Takeda Medical Science Foundation (to H. S.).

[S] The on-line version of this article (available at http://www.jbc.org) contains supplemental Table 1 and Figs. 1–8.

[1] Both authors contributed equally to this work.

[2] To whom correspondence should be addressed: Diabetes Research Center, Research Institute, National Center for Global Health and Medicine, 1-21-1 Toyama, Shinjuku-ku, Tokyo 162-8655, Japan. Tel.: 81-3-5273-6844; Fax: 81-3-5273-4526; E-mail: kasuga@ri.ncgm.go.jp.

[3] The abbreviations used are: WAT, white adipose tissue; BAT, brown adipose tissue; NBT, nitro blue tetrazolium; 8-OHdG, 8-hydroxy-2′-deoxyguanosine; ROS, reactive oxygen species; CM-H_2DCFDA, 5-(and-6)-chloromethyl-2′, 7′-dichlorodihydrofluorescein diacetate, acetyl ester; UCP, uncoupling protein; TBARS, thiobarbituric acid-reactive substances; Tg, transgenic.

liver and adipose tissue (15, 16) are resistant to the development of obesity induced by a high fat diet. However, mice with liver-specific ablation of SCD1 are not protected from high fat diet-induced obesity (17), suggesting that SCD1 in adipose tissue plays a key role in the development of obesity.

We have now investigated the role of KLF15 in adipose tissue (WAT and BAT) *in vivo* by generating transgenic mice in which KLF15 is overexpressed specifically in white and brown adipocytes. Our observations indicate that KLF15 suppresses the expression of SCD1 in adipose tissue. Moreover, this effect appears to influence pancreatic β cells, resulting in increased insulin secretion. Such signaling from adipose tissue to pancreatic β cells may contribute to the pathogenesis of type 2 diabetes induced by obesity.

EXPERIMENTAL PROCEDURES

Antibodies and Other Reagents—Antibodies to p42/44 MAPK, to phosphorylated Akt (Ser^{473}), to Akt, to α-tubulin, and to β-actin were obtained from Cell Signaling (Beverly, MA); those to SCD1 and those to KLF15 for immunoprecipitation were from Santa Cruz Biotechnology (Santa Cruz, CA); those to insulin receptor substrate-1 (IRS-1) and to phosphotyrosine were from Upstate Biotechnology, Inc. (Lake Placid, NY); and those to KLF15 for immunoblot analysis were generated as described previously (10). Adenoviruses encoding rat KLF15 or β-galactosidase were generated as described previously (5).

Generation of Adipose Tissue-specific KLF15 or SCD1 Transgenic Mice—We obtained a cDNA for rat KLF15 as described previously (5) and a cDNA for mouse SCD1 from Invitrogen. These cDNAs were subcloned separately and consecutively into the plasmids pCMV5-aP2 (kindly provided by B. M. Spiegelman, Dana-Farber Cancer Institute, Boston) and pBST-N (kindly provided by J. Miyazaki, Osaka University, Osaka, Japan). The final transgene constructs contained a 5.4-kb promoter-enhancer fragment of the mouse aP2 gene, the second intron of the rabbit β-globin gene, rat KLF15 or mouse SCD1 cDNA, and polyadenylation signals of the rabbit β-globin gene and SV40 early gene (18). These constructs were linearized and microinjected into pronuclear oocytes of C57BL/6 mice for the generation of chimeric mice. The resulting offspring were screened for transgene transmission by PCR analysis and Southern blot hybridization.

Animal Studies, Including Glucose and Insulin Tolerance Tests, and Dissections—Male mice were used for experiments. For examination of the effects of a high fat diet, mice were fed from 6 weeks of age with such a diet as described previously (19). Mice were deprived of food for 16 h before intraperitoneal injection of glucose (2 g/kg of body mass) for a glucose tolerance test, with blood samples being collected at various times (0–120 min) during the test. An insulin tolerance test was performed with mice in the randomly fed state; plasma glucose concentration was determined at various times (0–60 min) after intraperitoneal injection of human regular insulin (1.5 units/kg). For immunoprecipitation and immunoblot analysis of insulin-induced tyrosine phosphorylation of IRS-1 and serine phosphorylation of Akt, tissues were isolated from mice that had been deprived of food for 16 h and then stimulated with human regular insulin (0.5 units/kg) for 2 min. Tissue lysates were subjected to immunoprecipitation followed by immunoblot analysis as described previously (20). All experimental protocols with mice were approved by the animal ethics committees of Kobe University Graduate School of Medicine and the National Center for Global Health and Medicine. We carried out the sampling of fat depots as described previously (21). Specific definitions of dissected fat depots are as follows: epididymal WAT, prominent bilateral intra-abdominal visceral depots in male mice attached to the epididymides; subcutaneous WAT, bilateral superficial subcutaneous WAT depots between the skin and muscle fascia just anterior to the lower segment of the hind limbs; BAT, most prominent depot of classic brown adipocytes in rodents, found as bilobed tissue between the scapulae.

Measurement of Oxygen Consumption, Daily Food Intake, and Locomotor Activity—For measurement of O_2 consumption in mice, each animal was monitored individually in a metabolic cage (Oxymax; Columbus Instruments, Columbus, OH) with free access to food and drinking water. Each cage was monitored for both O_2 consumption and CO_2 production at 10-min intervals. Oxygen consumption and CO_2 production were expressed as milliliters of O_2 or CO_2/kg of body mass/h. For measurement of food intake and locomotor activity, mice were monitored individually in a cage with the ACTIMO system (Shinfactory, Fukuoka, Japan). This system measures locomotor activity with the use of infrared beams as well as food intake at 30-min intervals with the use of a top-loader balance. Oxygen consumption by isolated adipocytes was measured as described previously (22).

Analysis of Metabolic Parameters—Plasma glucose and insulin as well as serum leptin concentrations were measured as described previously (19). Serum levels of adiponectin, nonesterified fatty acids, and triglyceride were also measured as described previously (22). We extracted hepatic triglycerides using chloroform/methanol and determined levels by colorimetric assay as described above.

Isolation of Total RNA, RT-PCR Analysis, Northern Hybridization, and Quantification of Mitochondrial Copy Number—Total RNA was isolated from tissues and cells with the use of an RNeasy kit (Qiagen, Valencia, CA) and was subjected to reverse transcription using a high capacity cDNA reverse transcription kit (Applied Biosystems, Foster City, CA). The resulting cDNA was subjected to real time PCR analysis with a StepOnePlus instrument and SYBR Green Master Mix (Applied Biosystems). The relative abundance of mRNAs was calculated with 18 S rRNA as the invariant control. Northern blot analysis was performed as described previously (5) with a full-length mouse KLF15 cDNA or a fragment of mouse SCD1 cDNA as the probe. A probe for 28 S rRNA was used as a loading control. Quantification of mitochondrial copy number was performed as described previously (23, 24). In brief, DNA was isolated from whole tissue lysates and then subjected to real time PCR analysis with primers targeted to the mitochondrial gene for cytochrome *c* oxidase subunit I (COXI) and to the nuclear gene for 18 S rRNA. The ratio of the number of DNA copies for the COXI gene to that for the 18 S rRNA gene represents the rela-

tive mitochondrial copy number. Primers for all PCR analyses are listed in supplemental Table 1.

Cell Culture and Measurement of Insulin Secretion—3T3-L1 preadipocytes were maintained and induced to differentiate into white adipocytes as described previously (5). HB2 cells (kindly provided by M. Saito, Tenshi College, Sapporo, Japan) were also maintained and induced to differentiate into brown adipocytes as described previously (22). MIN6 cells (kindly provided by S. Seino, Kobe University, Kobe, Japan) were maintained as described previously (25). 3T3-L1 adipocytes were infected with recombinant adenoviruses at 5 days after the induction of differentiation, and the medium was changed daily until the initiation of coculture with MIN6 cells at 7 days after the induction of differentiation. The two cell types in the coculture were separated by a nylon filter with a pore size of 3 μm. After coculture for 2 days, the cells were incubated at 37 °C first for 30 min in HEPES-buffered Krebs-Ringer solution (119 mM NaCl, 1.19 mM KH_2PO_4, 1.19 mM $MgSO_4$, 2.54 mM $CaCl_2$, and 10 mM HEPES (pH 7.4)) supplemented with 2% BSA and 2.8 mM glucose and then for 2 h in the same solution supplemented with 2% BSA and either 2.8 or 16.8 mM glucose. Insulin released into the medium by MIN6 cells was measured as described above and was normalized by the cellular protein content.

Measurement of Oxidative Stress—The nitro blue tetrazolium (NBT) assay was performed as described previously (26). The levels of lipid peroxidation in plasma and in tissue homogenates were measured with a TBARS Assay kit (Cayman, Ann Arbor, MI). Urinary 8-hydroxy-2′-deoxyguanosine (8-OHdG) excretion was measured with an ELISA kit (Japan Institute for the Control of Aging, Shizuoka, Japan). Experiments with the reactive oxygen species (ROS)-sensitive fluorescent dye 5-(and-6)-chloromethyl-2′,7′-dichlorodihydrofluorescein diacetate, acetyl ester (CM-H_2DCFDA), were performed essentially as described previously (27). Hydroperoxy forms of triglyceride and phosphatidylcholine were quantitated with the use of reversed-phase liquid chromatography and electrospray ionization-MS as described previously (28).

Immunoblot Analysis, Immunoprecipitation, and ChIP—Immunoblot analysis was performed as described previously (5). For immunoprecipitation, tissue lysates were assayed for protein content with a BCA protein assay kit (Thermo Scientific, Rockford, IL), and equal amounts of lysate protein (480 μg) were then incubated overnight at 4 °C in a total volume of 400 μl with 1 μg of antibodies to KLF15 that had been bound to protein G-Sepharose beads (GE Healthcare). The resulting immunoprecipitates were washed three times with wash buffer (50 mM Tris-HCl (pH 7.5), 1% Nonidet P-40, 150 mM NaCl, 2 mM EGTA), suspended in SDS sample buffer, boiled for 4 min, and subjected to SDS-PAGE on a 10% gel followed by immunoblot analysis. ChIP analysis was performed with the use of a ChIP assay kit (Upstate Biotechnology, Inc.). In brief, cells were incubated for 30 min at room 37 °C with 1% formaldehyde in culture medium, washed with ice-cold PBS, and subjected to ultrasonic treatment in SDS lysis buffer (kit component) containing aprotinin (1 μg/ml) and leupeptin (1 μg/ml). The cell lysates were incubated overnight at 4 °C with antibodies to KLF15 or normal goat IgG, after which protein A-agarose was added, and each mixture was incubated for an additional 1 h. The precipitated DNA-protein complexes were washed, eluted from the agarose beads, and dissociated. DNA was then extracted with phenol/chloroform and used as a template for PCR analysis with the primers 5′-GGAATCACGTTATCCTGC-3′ (sense) and 5′-GCTAATGTGCCTCCTGTG-3′ (antisense).

Luciferase Reporter Assays—3T3-L1 adipocytes or HB2 cells in 10-cm dishes were transfected with 1 μg of pGL3-basic (Promega, Madison, WI) containing (or not) a fragment of the mouse SCD1 gene promoter (nucleotides −669 to +157 relative to the transcription initiation site), 2 μg of pcDNA3.1 containing rat KLF15 cDNA (pcDNA3.1/KLF15) or the empty vector, and 0.3 μg of pRL-TK (Promega) by electroporation as described previously (5). After 48 h, the cells were lysed in Passive Lysis Buffer (Promega), and portions of the lysates were assayed for firefly and *Renilla* luciferase activities with the use of a Dual-Luciferase assay system (Promega). Promoter activity was determined as the ratio of firefly to *Renilla* luciferase activities.

Determination of Adipocyte Size and β Cell Area—Adipocyte size was determined with a Coulter counter as described previously (19). The area of β cells was determined by hematoxylin-eosin staining of pancreatic sections as described previously (29).

Statistical Analysis—Data are presented as means ± S.E. Differences between two groups were evaluated by Student's unpaired two-tailed *t* test as performed with StatView software (SAS Institute, Cary, NC). A p value of <0.05 was considered statistically significant.

RESULTS

Down-regulation of KLF15 in WAT and BAT of Obese Mice and Generation of Adipose Tissue-specific KLF15 Transgenic Mice—We first examined the expression of KLF15 in (epididymal) WAT and BAT of obese mice. In both C57BL/6 mice fed a high fat diet and genetically obese diabetic (db/db) mice, the expression of KLF15 in WAT and BAT was reduced at both the mRNA and protein levels compared with control mice (Fig. 1, *A* and *B*). To investigate the role of KLF15 in adipose tissue *in vivo*, we next generated adipose tissue-specific KLF15 transgenic (aP2-KLF15 Tg) mice in which KLF15 is expressed under the control of a 5.4-kb promoter-enhancer fragment of the mouse aP2 gene. We obtained three lines of such transgenic mice, two of which (1Tg and 3Tg) were examined further. Northern blot and RT and real time PCR analyses confirmed that both 1Tg and 3Tg lines expressed the transgene almost exclusively in adipose tissue (Fig. 1*C* and supplemental Fig. 1). The abundance of KLF15 mRNA in WAT of the 1Tg and 3Tg lines fed normal chow was 1.4 and 2.4 times, respectively, that in WT littermates (supplemental Fig. 2). However, for mice fed a high fat diet, the amount of KLF15 mRNA in WAT of the 1Tg and 3Tg lines was increased to a greater extent (3.7- and 22.6-fold, respectively, compared with WT controls) (supplemental Fig. 2). The amount of KLF15 mRNA in BAT of the 1Tg and 3Tg lines was increased 2.9 and 3.6 times, respectively, for mice fed normal chow and 7.4 and 16.4 times, respectively, for those fed a high fat diet (supplemental Fig. 2).

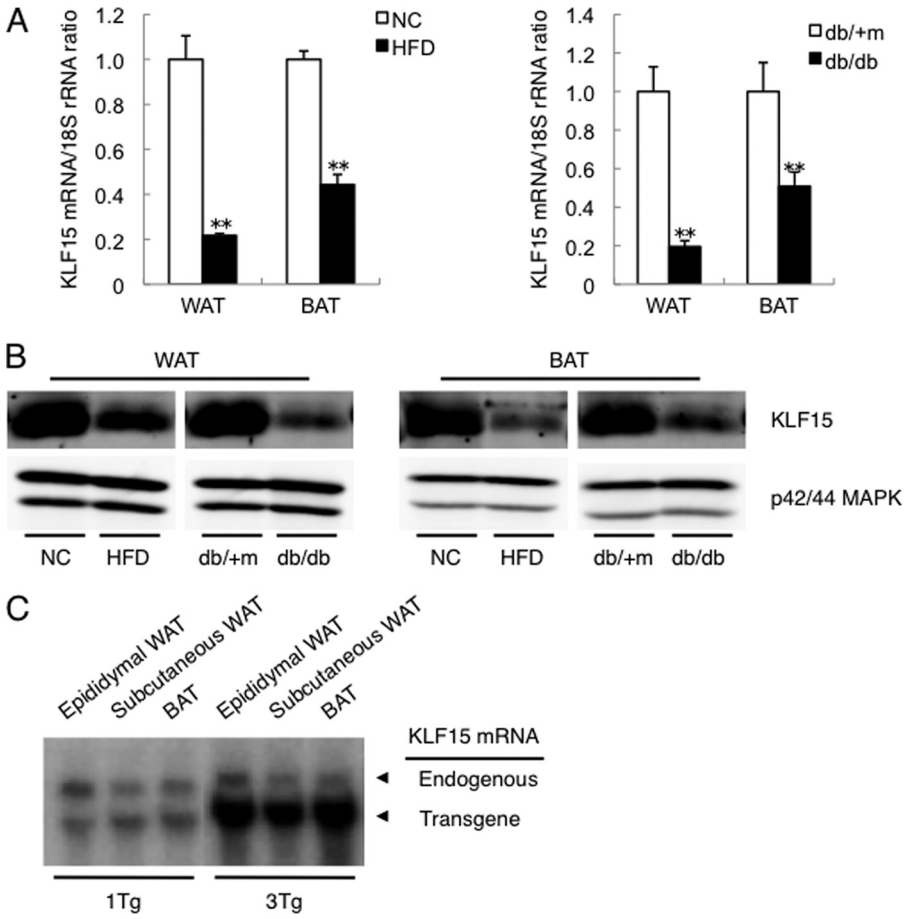

FIGURE 1. **Down-regulation of KLF15 expression in adipose tissue of obese mice and generation of adipose tissue-specific KLF15 transgenic mice.** *A,* amount of KLF15 mRNA in (epididymal) WAT or BAT of 23-week-old C57BL/6 mice fed normal chow (*NC*) or a high fat diet (*HFD*) (*left panel*) as well as in 23-week-old db/+m (control) and db/db (genetically obese diabetic) mice (*right panel*) was examined by RT and real time PCR analysis. Quantitative data are normalized by the abundance of 18 S rRNA, are expressed relative to corresponding value for control mice, and are means ± S.E. for five mice. **, $p < 0.01$ *versus* control mice. *B,* whole lysates of WAT or BAT of mice as in *A* were subjected to immunoprecipitation and immunoblot analysis with antibodies to KLF15 or to direct immunoblot analysis with antibodies to p42/44 MAPK (loading control). *C,* Northern blot analysis of KLF15 mRNA (endogenous and transgene-derived) in various fat depots of aP2-KLF15 Tg mice (1Tg and 3Tg lines) at 23 weeks of age. Data in *B* and *C* are representative of at least three independent experiments.

Resistance to Diet-induced Obesity, Insulin Resistance, and Improved Glucose Tolerance in aP2-KLF15 Tg Mice—Animals of both lines (1Tg and 3Tg) of aP2-KLF15 Tg mice were born in a Mendelian ratio and appeared physically normal at birth. Body mass also did not differ between aP2-KL15 Tg and WT littermates maintained on normal chow (Fig. 2*A*). However, when fed a high fat diet, aP2-KLF15 Tg mice were significantly leaner than WT littermates in a manner dependent on transgene dosage (Fig. 2*A*). We therefore performed subsequent examinations with mice fed a high fat diet. The mass of WAT was also reduced in aP2-KLF15 Tg mice in a transgene dosage-dependent manner, whereas the mass of the liver was increased (supplemental Fig. 3*A*). Consistent with the observed decrease in WAT mass, the size of white adipocytes was smaller in aP2-KLF15 Tg mice of both lines than in WT littermates (supplemental Fig. 3*B*).

We next investigated glucose metabolism in aP2-KLF15 Tg mice. The plasma insulin concentration in the fed state was increased in these animals, whereas the plasma glucose concentration did not differ from that in WT controls (Table 1). Furthermore, plasma glucose levels during an intraperitoneal insulin tolerance test were significantly higher in aP2-KLF15 Tg mice than in WT littermates (Fig. 2*B*), indicative of insulin resistance in the former animals. We therefore examined insulin signaling in the liver and skeletal muscle of aP2-KLF15 Tg mice. The phosphorylation of IRS-1 on tyrosine residues and that of Akt on Ser^{473}, both of which are key events in insulin signaling, was attenuated in both the liver and skeletal muscle of aP2-KLF15 Tg mice, whereas the total abundance of these proteins did not differ between the two genotypes (Fig. 2*C*). Consistent with the increased liver mass and impaired hepatic insulin resistance, hepatic triglyceride accumulation is more severe in 3Tg mice compared with controls (Fig. 2*D*). Unexpectedly, despite their insulin resistance, an intraperitoneal glucose tolerance test revealed that aP2-KLF15 Tg mice were more glucose tolerant than were WT littermates (Fig. 2*E*). Insulin secretion during the glucose tolerance test was more pronounced in aP2-KLF15 Tg mice than in the WT controls (Fig. 2*F*). Examination of islet morphology also revealed that the area occupied by β cells in the pancreas was significantly greater in aP2-KLF15 Tg mice than in WT littermates (supplemental Fig. 4). These various observations thus suggested that aP2-KLF15 Tg mice show improved glucose tolerance as a result of increased insulin secretion. Also of note, the serum adiponectin level was signif-

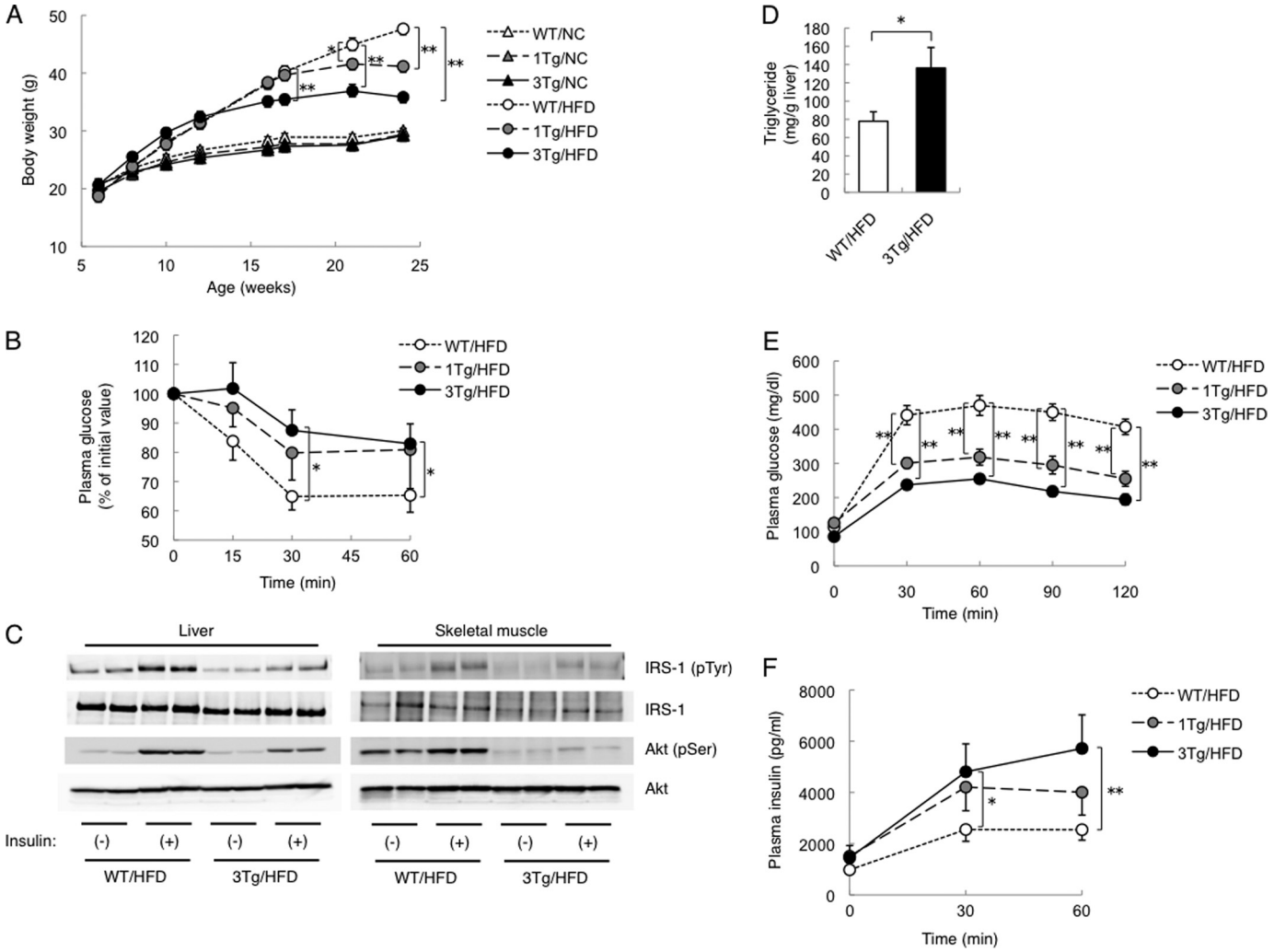

FIGURE 2. **Metabolic characteristics of adipose tissue-specific KLF15 transgenic mice.** *A,* time course of body mass for WT and aP2-KLF15 Tg (1Tg and 3Tg) mice fed normal chow (*NC*) or a high fat diet (*HFD*). Data are means ± S.E. for 15 mice. *, $p < 0.05$; **, $p < 0.01$. *B,* glucose clearance during an insulin tolerance test in 17-week-old WT and aP2-KLF15 Tg mice fed a high fat diet. Plasma glucose concentration is expressed relative to the initial value. Data are means ± S.E. for 8–12 mice. *, $p < 0.05$. *C,* insulin-induced tyrosine phosphorylation of IRS-1 and Ser^{473} phosphorylation of Akt in the liver and skeletal muscle of 17-week-old WT and aP2-KLF15 Tg mice fed a high fat diet. Immunoprecipitates prepared with antibodies to IRS-1 or to Akt were subjected to immunoblot analysis with antibodies to phosphotyrosine and to IRS-1 or with those to Ser^{473}-phosphorylated or total forms of Akt, respectively. *D,* hepatic triglyceride contents in 23-week-old WT and aP2-KLF15 Tg mice fed a high fat diet. Data are means ± S.E. for 8 mice. *, $p < 0.01$. *E* and *F*, plasma glucose (*E*) and plasma insulin (*F*) concentrations during an intraperitoneal glucose tolerance test in 21-week-old WT and aP2-KLF15 Tg mice fed a high fat diet. Data are means ± S.E. for 8–12 mice. *, $p < 0.05$; **, $p < 0.01$. Data in *E* are representative of at least three independent experiments.

TABLE 1

Metabolic parameters of WT and aP2-KLF15 Tg mice

The plasma concentrations of glucose and insulin as well as the serum concentrations of leptin, adiponectin, nonesterified fatty acids (NEFA), and triglyceride were determined in 23-week-old WT and aP2-KLF15 Tg (1Tg and 3Tg) mice maintained on a high fat diet in the randomly fed state. Data are means ± S.E. for 10 mice.

Parameter	WT/HFD	1Tg/HFD	3Tg/HFD
Glucose	165.0 ± 6.9 mg/dl	173.5 ± 8.2 mg/dl	184.5 ± 18.0 mg/dl
Insulin	6.1 ± 1.2 ng/ml	17.0 ± 9.6 ng/ml	39.9 ± 14.9 ng/ml[a]
Leptin	117.6 ± 14.9 ng/ml	84.2 ± 8.6 ng/ml[a]	14.7 ± 2.3 ng/ml[a]
Adiponectin	23.8 ± 1.4 μg/ml	19.9 ± 1.8[b]	5.81 ± 0 μg/ml[a]
NEFA	1.021 ± 0.082 mEq/liter	0.879 ± 0.077 mEq/liter	0.757 ± 0.062 mEq/liter[b]
Triglyceride	76.3 ± 8.2 mg/dl	73.8 ± 9.4 mg/dl	81.1 ± 13.9 mg/dl

[a] $p < 0.01$ *versus* WT mice.
[b] $p < 0.05$ *versus* WT mice.

icantly lower in aP2-KLF15 Tg mice than in WT littermates (Table 1), despite the relative leanness of the former animals.

Increased O_2 Consumption in aP2-KLF15 Tg Mice—Given that aP2-KLF15 Tg mice remained relatively lean on a high fat diet, we measured O_2 consumption, the respiratory quotient, food intake, and locomotor activity for these animals. Oxygen consumption by aP2-KLF15 Tg mice was significantly increased compared with WT littermates, whereas the respiratory quotient, food intake, and locomotor activity did not differ between the two genotypes (Fig. 3*A*). Furthermore, O_2 consumption under both basal and epinephrine-stimulated conditions was increased for white and brown adipocytes isolated

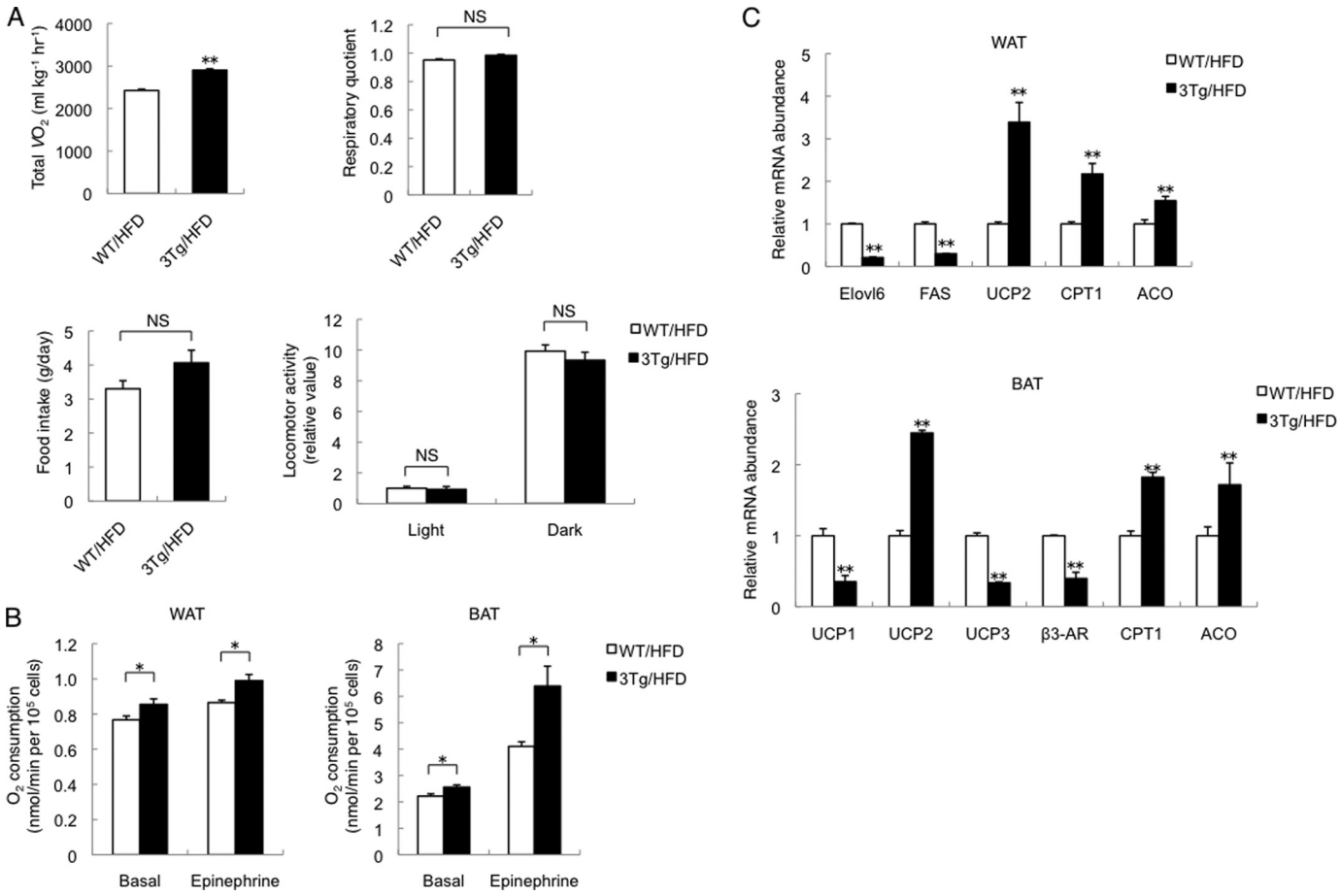

FIGURE 3. **Increased O_2 consumption by adipocytes overexpressing KLF15.** *A,* total O_2 consumption (VO_2), respiratory quotient, daily food intake, and locomotor activity in the light (12 h) and dark (12 h) phases for 23-week-old WT and aP2-KLF15 Tg (3Tg) mice fed a high fat diet (*HFD*). Data are means ± S.E. for five mice. **, $p < 0.01$ *versus* WT controls; *NS,* not significant. *B,* oxygen consumption by adipocytes isolated from WAT or BAT of 23-week-old WT and aP2-KLF15 Tg mice fed a high fat diet. The isolated adipocytes were incubated in the absence or presence of epinephrine (100 nM). Data are means ± S.E. for four mice. *, $p < 0.05$. *C,* RT and real time PCR analysis of mRNAs for the indicated proteins in WAT and BAT of 23-week-old WT and aP2-KLF15 Tg mice fed a high fat diet. *β3-AR*, β_3-adrenergic receptor. Data are normalized by the abundance of 18 S rRNA, are expressed relative to the corresponding value for WT mice, and are means ± S.E. for five mice. **, $p < 0.01$ *versus* WT controls.

from aP2-KLF15 Tg mice compared white and brown adipocytes isolated from WT controls (Fig. 3*B*). However, mitochondrial copy number was reduced in both WAT and BAT of aP2-KLF15 Tg mice (supplemental Fig. 5), suggesting that the increased O_2 consumption by white and brown adipocytes of these mice results from increased mitochondrial function or peroxisomal β-oxidation. To investigate these possibilities, we examined the expression of various genes in WAT and BAT of aP2-KLF15 Tg and WT mice. We found that the amounts of mRNAs for carnitine palmitoyltransferase 1 (CPT1), which controls the entry of long chain fatty acyl-CoA into mitochondria, and for acyl-CoA oxidase, a key enzyme of β-oxidation in peroxisomes, were increased in WAT of aP2-KLF15 Tg mice (Fig. 3*C*). Moreover, the amounts of mRNAs encoding enzymes for lipid synthesis such as elongation of long chain fatty acids family member 6 (Elovl6) and fatty-acid synthase were decreased in WAT of aP2-KLF15 Tg mice (Fig. 3*C*). The abundance of the mRNA for uncoupling protein 2, the major uncoupling protein in WAT, was increased in WAT of aP2-KLF15 Tg mice (Fig. 3*C*), although the mRNA expression of UCP1 and PGC1α, two representative genes abundant in BAT, was not up-regulated, suggesting no conversion of the WAT to BAT (supplemental Fig. 6). With regard to BAT, the amounts of mRNAs for CPT1 and acyl-CoA oxidase were also increased in aP2-KLF15 Tg mice compared with WT littermates (Fig. 3*C*). These data thus suggested that overexpression of KLF15 in white and brown adipose tissue affects the expression of genes important for mitochondrial function and peroxisomal β-oxidation and thereby increases O_2 consumption by white and brown adipocytes.

Down-regulation of SCD1 in Adipocytes Overexpressing KLF15—To identify other genes regulated by KLF15 in adipocytes, we analyzed total RNA isolated from WAT or BAT of both aP2-KLF15 Tg mice and WT littermates with mouse oligonucleotide microarrays. We searched for genes related to glucose metabolism whose expression was increased or decreased in a manner dependent on transgene dosage in mice maintained on a high fat diet. Such analysis revealed that expression of the SCD1 gene was decreased in a transgene dosage-dependent manner (data not shown). RT and real time PCR analysis confirmed that the amount of SCD1 mRNA in WAT and BAT of aP2-KLF15 Tg mice fed a high fat diet was decreased in a manner dependent on transgene dosage (Fig. 4*A*). The abundance of SCD1 mRNA in the liver (another

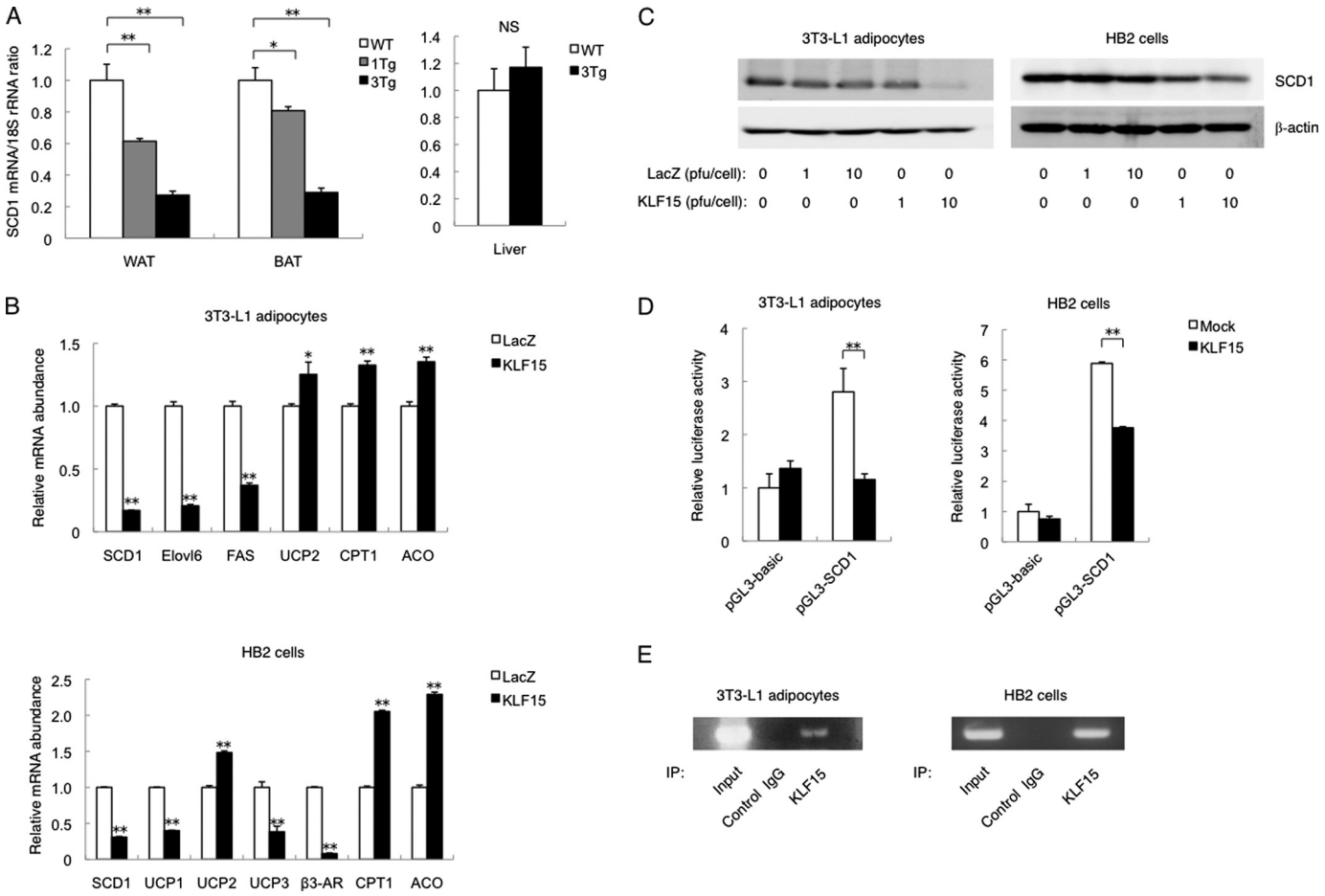

FIGURE 4. **Down-regulation of SCD1 expression in adipocytes overexpressing KLF15.** *A,* RT and real time PCR analysis of SCD1 mRNA in WAT, BAT, and the liver of 23-week-old WT and aP2-KLF15 Tg (1Tg and 3Tg) mice fed a high fat diet. Data are normalized by the abundance of 18 S rRNA, are expressed relative to the corresponding value for WT mice, and are means ± S.E. for five mice. *, $p < 0.05$; **, $p < 0.01$; *NS,* not significant. *B,* RT and real time PCR analysis of mRNAs for the indicated proteins in 3T3-L1 adipocytes and HB2 cells infected with adenoviruses encoding either KLF15 or β-galactosidase (*LacZ*) at a multiplicity of infection of 10 pfu/cell. The cells were infected with adenoviruses at 5 days after the induction of differentiation and were analyzed 48 h later. Data are normalized by the abundance of 18 S rRNA, are expressed relative to the corresponding control value, and are means ± S.E. from three independent experiments. *, $p < 0.05$; **, $p < 0.01$ *versus* control (*LacZ*). *C,* immunoblot analysis of SCD1 and β-actin (loading control) in 3T3-L1 adipocytes and HB2 cells infected with adenoviruses at the indicated multiplicities of infection as in *B*. *D,* 3T3-L1 adipocytes and HB2 cells at 5 days after the induction of differentiation were transfected with a luciferase reporter plasmid containing a fragment of the SCD1 gene promoter (*pGL3-SCD1*) or the corresponding empty vector (*pGL3-basic*), with pRL-TK, and with an expression vector for KLF15 or the corresponding empty vector (pcDNA3.1, *Mock*). After 48 h, the cells were assayed for luciferase activities, and firefly luciferase activity was normalized by *Renilla* luciferase activity. Data are expressed relative to the value for cells transfected with pGL3-basic and pcDNA3.1 and are means ± S.E. of triplicates from an experiment that was repeated a total of three times with similar results. **, $p < 0.01$. *E,* ChIP assay of the binding of KLF15 to the SCD1 gene promoter in 3T3-L1 adipocytes and HB2 cells. The cells were subjected to immunoprecipitation (*IP*) with antibodies to KLF15 or with control IgG at 7 days after the induction of differentiation. The resulting immunoprecipitates as well as total cell lysates (*Input*) were then processed for PCR analysis. Data in *C* and *E* are representative of three independent experiments.

important site of SCD1 expression) did not differ significantly between aP2-KLF15 Tg mice and WT littermates (Fig. 4*A*).

The transgene expression in aP2-KLF15 Tg mice was detected not only in adipose tissues, but also in macrophage (supplemental Fig. 1). To confirm that these changes in gene expression in adipocytes overexpressing KLF15 *in vivo* were cell autonomous, we infected 3T3-L1 adipocytes and HB2 cells, which are mouse white and brown adipocyte cell lines, respectively, with a recombinant adenovirus encoding KLF15. The expression of SCD1 was decreased at both the mRNA and protein levels in both 3T3-L1 adipocytes and HB2 cells overexpressing KLF15 (Fig. 4, *B* and *C*). The expression of genes related to mitochondrial function or peroxisomal β-oxidation in 3T3-L1 adipocytes and HB2 cells was affected by KLF15 overexpression in a manner similar to that observed with WAT and BAT, respectively, *in vivo*. In addition, KLF15 inhibited the activity of the SCD1 gene promoter in both cell lines (Fig. 4*D*). Furthermore, ChIP analysis revealed that endogenous KLF15 was bound to the promoter region of the SCD1 gene in both 3T3-L1 adipocytes and HB2 cells (Fig. 4*E*). These data thus suggested that KLF15 binds to the promoter of the SCD1 gene and thereby represses its transcription in white and brown adipocytes.

Decreased Oxidative Stress in Adipocytes Overexpressing KLF15—We next examined the mechanism responsible for the increased insulin secretion observed in aP2-KLF15 Tg mice. To determine whether this increased secretion might reflect a direct effect of adipocytes on β cells, we performed coculture experiments. Glucose-stimulated insulin secretion from MIN6 cells (mouse β cell line) cocultured with 3T3-L1 adipocytes infected with an adenovirus encoding KLF15 was significantly increased compared with cells cocultured with 3T3-L1 adipocytes infected with a control adenovirus (Fig. 5*A*), suggesting

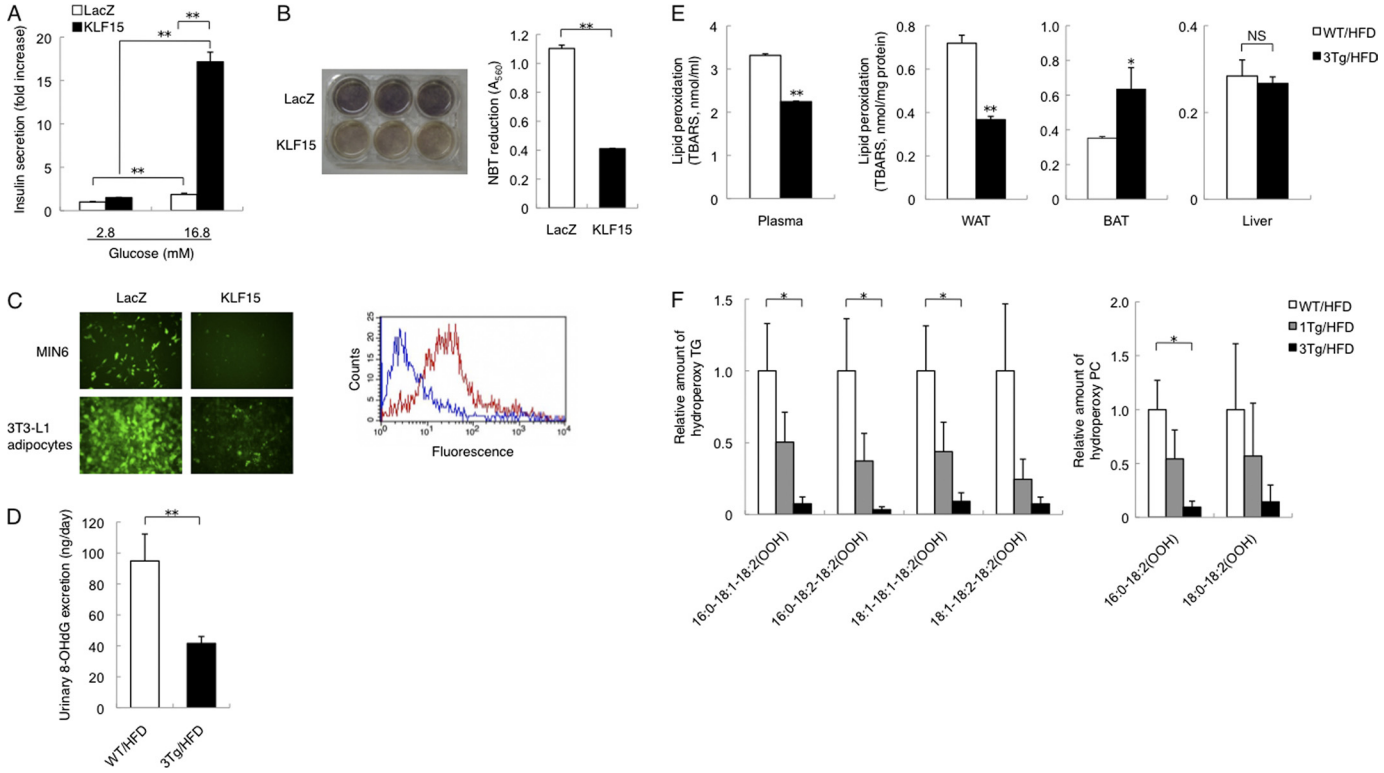

FIGURE 5. **Decreased oxidative stress in adipocytes overexpressing KLF15.** *A,* MIN6 cells cocultured with 3T3-L1 adipocytes were assayed for insulin secretion in the presence of 2.8 or 16.8 mM glucose. The two cell types were separated by a nylon filter with a pore size of 3 μm. Before coculture, the 3T3-L1 adipocytes were infected with adenoviruses encoding KLF15 or β-galactosidase (*LacZ*). Data are expressed as fold increase relative to the value for MIN6 cells cocultured with LacZ-expressing 3T3-L1 adipocytes and exposed to 2.8 mM glucose, and they are means ± S.E. of triplicates from an experiment that was repeated a total of three times with similar results. **, $p < 0.01$. *B,* oxidative stress in 3T3-L1 adipocytes infected with adenoviruses encoding KLF15 or β-galactosidase. Oxidative stress was measured with the NBT assay, in which NBT (*yellow*) is reduced by superoxide to formazan (*dark blue*). Cells treated with NBT are shown in the *left panel*, and the absorbance of the dissolved formazan product at 560 nm was measured (*right panel*). Quantitative data are means ± S.E. of triplicates from an experiment that was repeated a total of three times with similar results. **, $p < 0.01$. *C,* oxidative stress in MIN6 cells and 3T3-L1 adipocytes. MIN6 cells were cocultured for 48 h with 3T3-L1 adipocytes infected with adenoviruses encoding KLF15 or β-galactosidase, after which oxidative stress in the two cell types was evaluated with the ROS-sensitive fluorescent dye CM-H_2DCFDA. Representative fluorescence images of MIN6 cells and 3T3-L1 adipocytes are shown in the *left panel*, and a representative histogram for flow cytometric analysis of fluorescence in MIN6 cells (*red line*, LacZ; *blue line*, KLF15) is shown in the *right panel*. Data are representative of three independent experiments. *D,* urinary 8-OHdG excretion by 23-week-old WT and aP2-KLF15 Tg (*3Tg*) mice fed a high fat diet (*HFD*). Data are means ± S.E. for five mice. **, $p < 0.01$. *E,* plasma and tissue levels of lipid peroxidation evaluated from the formation of TBARS for 23-week-old WT and aP2-KLF15 Tg mice fed a high fat diet. Data are means ± S.E. for five mice. *, $p < 0.05$; **, $p < 0.01$ *versus* WT mice; *NS*, not significant. *F,* reversed-phase liquid chromatography and electrospray ionization-MS analysis of hydroperoxy (*OOH*) forms of triglyceride and phosphatidylcholine with the indicated fatty acid compositions in WAT of 23-week-old WT and aP2-KLF15 Tg (1Tg and 3Tg) mice fed a high fat diet. Data are expressed relative to the corresponding value for WT mice and are means ± S.E. for three mice. *, $p < 0.05$.

that adipocytes overexpressing KLF15 are able to increase insulin secretion from β cells.

Pancreatic β cells are more sensitive to oxidative stress compared with other tissues and cells (30–34), and oxidative stress is increased in the obese state, with the major source of oxidative stress associated with obesity being WAT (26). We therefore measured oxidative stress in adipocytes overexpressing KLF15. Oxidative stress, as reflected by the reduction of NBT, was significantly decreased in 3T3-L1 adipocytes infected with an adenovirus encoding KLF15 compared with 3T3-L1 adipocytes infected with a control adenovirus (Fig. 5*B*). In coculture experiments, oxidative stress, as evaluated with the ROS-sensitive dye CM-H_2DCFDA, was decreased in MIN6 cells cultured with KLF15-overexpressing 3T3-L1 adipocytes compared with MIN6 cells cultured with control 3T3-L1 adipocytes (Fig. 5*C*).

We next examined oxidative stress *in vivo*. Oxidative stress as reflected by the amount of urinary 8-OHdG, a biological marker of oxidative damage to DNA, was decreased in aP2-KLF15 Tg mice fed a high fat diet compared with WT littermates (Fig. 5*D*). Plasma lipid peroxidation, a biological marker of oxidative injury, was evaluated from the formation of TBARS and was also decreased in aP2-KLF15 Tg mice fed a high fat diet compared with WT littermates (Fig. 5*E*). To determine the site responsible for the reduced level of whole body oxidative stress in aP2-KLF15 Tg mice, we measured lipid peroxidation in WAT, BAT, and the liver. Lipid peroxidation in WAT was significantly decreased, whereas that in BAT was increased, and that in the liver was unaffected in aP2-KLF15 Tg mice on a high fat diet compared with WT controls (Fig. 5*E*). Moreover, examination of WAT by reversed-phase liquid chromatography and electrospray ionization-MS analysis revealed that the amount of hydroperoxy forms of triglyceride and phosphatidylcholine was decreased in a manner dependent on transgene dosage (Fig. 5*F*). These data thus suggested that a reduced level of oxidative stress in WAT results in a reduced level of whole body oxidative stress and thereby increases insulin secretion from pancreatic β cells in aP2-KLF15 Tg mice maintained on a high fat diet.

Restoration of SCD1 Expression in White Adipocytes Attenuates the Increased Insulin Secretion in aP2-KLF15 Tg Mice—The expression of SCD1 was down-regulated in WAT of aP2-

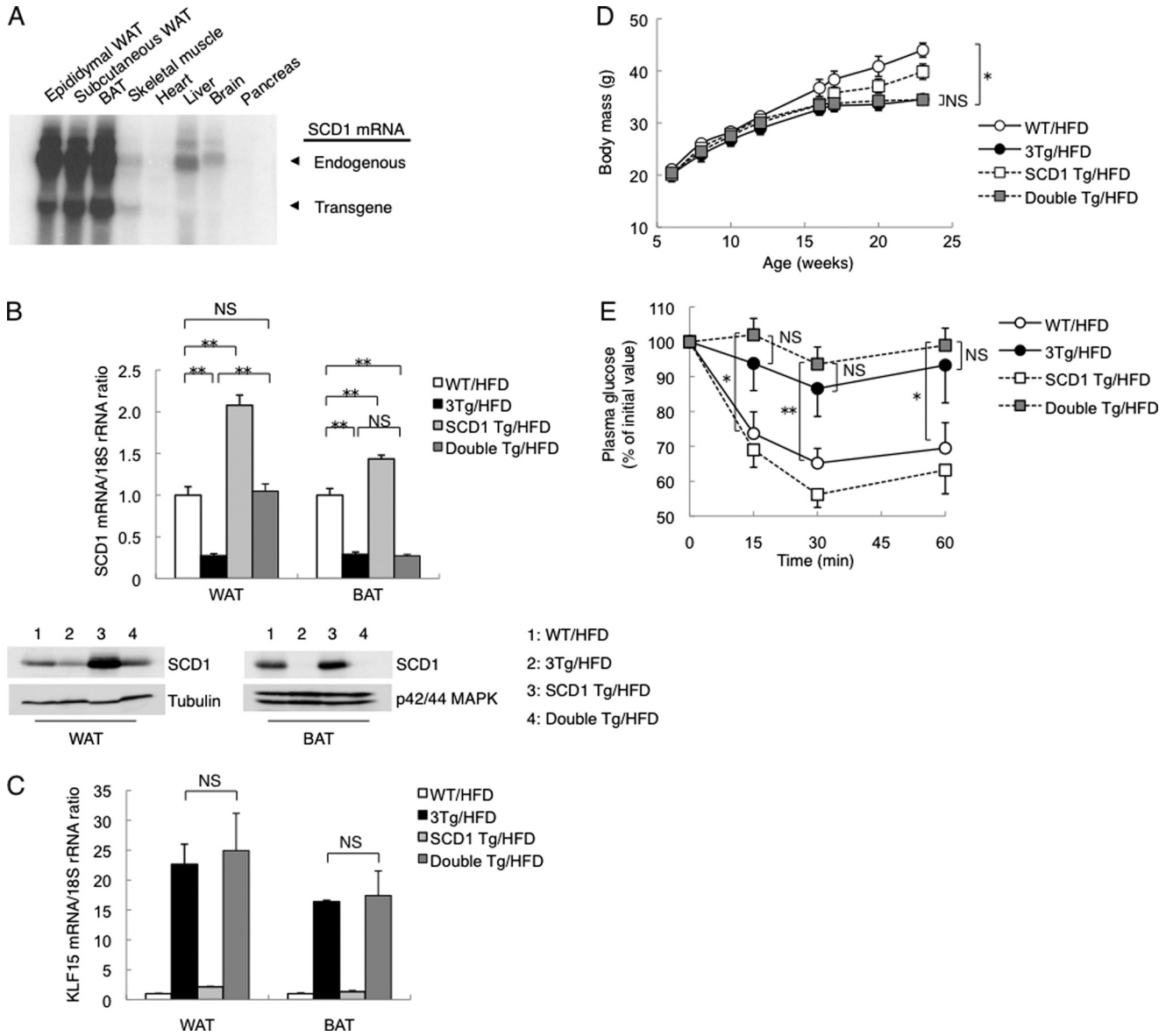

FIGURE 6. **Effects of transgenic restoration of SCD1 expression in adipocytes of aP2-KLF15 Tg mice.** *A,* Northern blot analysis of SCD1 mRNA (endogenous and transgene-derived) in various tissues of SCD1 Tg mice at 23 weeks of age. *B,* RT and real time PCR analysis of SCD1 mRNA (*upper panel*) as well as immunoblot analysis of SCD1 and of α-tubulin and p42/44 MAPK as loading controls (*lower panels*) in WAT and BAT of 23-week-old WT, aP2-KLF15 Tg (3Tg), SCD1 Tg, and double Tg mice fed a high fat diet (*HFD*). The mRNA data are normalized by the abundance of 18 S rRNA, are expressed relative to the corresponding value for WT mice, and are means ± S.E. for five mice. **, $p < 0.01$. *NS,* not significant. *C,* RT and real time PCR analysis of KLF15 mRNA in WAT and BAT of 23-week-old mice of the indicated genotypes fed a high fat diet. Data are normalized by the abundance of 18 S rRNA, are expressed relative to the corresponding value for WT mice, and are means ± S.E. for five mice. *D,* time course of body mass for mice of the indicated genotypes fed a high fat diet. Data are means ± S.E. for 10 mice. *, $p < 0.05$. *E,* glucose clearance during an insulin tolerance test in 17-week-old mice of the indicated genotypes maintained on a high fat diet. Plasma glucose concentration is expressed relative to the initial value. Data are means ± S.E. for eight mice. *, $p < 0.05$; **, $p < 0.01$. Data in *A* and *B* (*lower panels*) are representative of at least three independent experiments.

KLF15 Tg mice compared with WT littermates. To investigate whether this down-regulation of SCD1 was responsible for the reduced levels of oxidative stress in WAT and the entire body as well as for the increased insulin secretion in aP2-KLF15 mice, we generated adipose tissue-specific SCD1 transgenic mice (SCD1 Tg mice). To obtain adipose tissue-specific expression of the SCD1 transgene, we used the same promoter-enhancer fragment of the mouse aP2 gene as that used in the generation of aP2-KLF15 Tg mice. Northern blot analysis confirmed that SCD1 Tg mice expressed the transgene almost exclusively in WAT and BAT (Fig. 6*A* and supplemental Fig. 7). To restore the expression of SCD1 in adipose tissue of aP2-KLF15 Tg mice, we crossed aP2-KLF15 Tg (3Tg) mice with SCD1 Tg mice and obtained double transgenic (double Tg) mice. RT and real time PCR analysis as well as immunoblot analysis revealed that the amounts of SCD1 mRNA and protein in WAT of the double Tg mice maintained on a high fat diet were restored to the levels observed in WT littermates (Fig. 6*B*). However, the expression of SCD1 in BAT of double Tg mice fed a high fat diet remained lower than that in WT mice (Fig. 6*B*). The amounts of KLF15 mRNA in WAT and BAT of double Tg mice fed a high fat diet were similar to those apparent in 3Tg mice (Fig. 6*C*). These data thus indicated that the expression of SCD1 was restored only in WAT (not in BAT) of double Tg mice on a high fat diet.

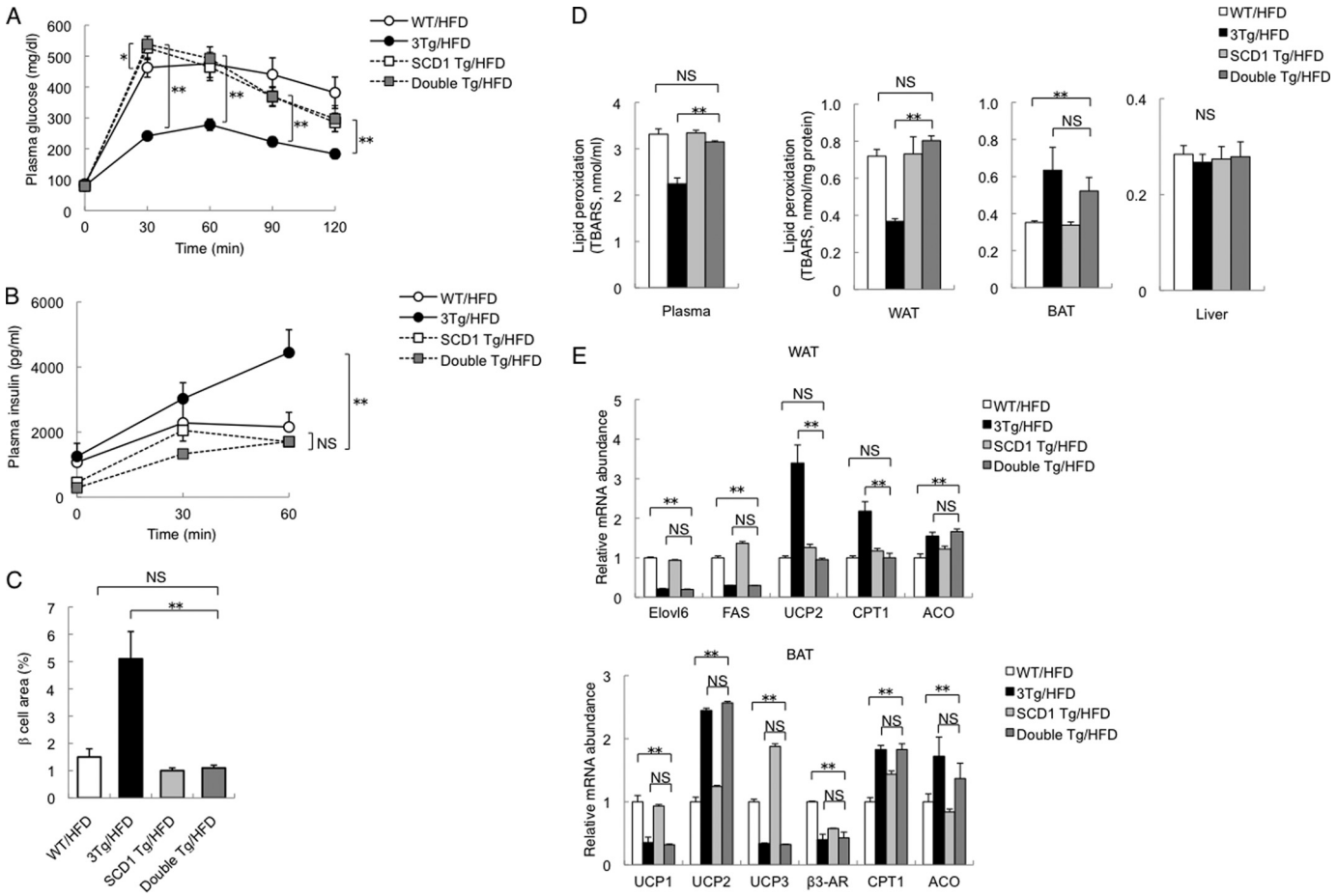

FIGURE 7. **Glucose metabolism and oxidative stress in double Tg mice.** *A* and *B*, plasma glucose (*A*) and plasma insulin (*B*) concentrations during an intraperitoneal glucose tolerance test in 21-week-old WT, aP2-KLF15 Tg (3Tg), SCD1 Tg, and double Tg mice maintained on a high fat diet (*HFD*). Data are means ± S.E. for 8 to 12 mice. *, $p < 0.05$; **, $p < 0.01$; *NS*, not significant. *C*, quantitation of β cell area as a percentage of total pancreatic area in 23-week-old mice of the indicated genotypes fed a high fat diet. Data are means ± S.E. for five mice. **, $p < 0.01$. *D*, plasma and tissue levels of lipid peroxidation evaluated from the formation of TBARS in 23-week-old mice of the indicated genotypes fed a high fat diet. Data are means ± S.E. for five mice. **, $p < 0.01$. *E*, RT and real time PCR analysis of mRNAs for the indicated proteins in WAT and BAT of 23-week-old mice of the indicated genotypes fed a high fat diet. Data are normalized by the abundance of 18 S rRNA, are expressed relative to the corresponding value for WT mice, and are means ± S.E. for five mice. **, $p < 0.01$. *ACO*, acyl-CoA oxidase.

There were no significant differences in body mass (Fig. 6*D*), in WAT mass (supplemental Fig. 8*A*), in white adipocyte size (supplemental Fig. 8*B*), in the serum concentration of adiponectin (supplemental Fig. 8*C*), or in plasma glucose levels during an intraperitoneal insulin tolerance test (Fig. 6*E*) between double Tg mice and 3Tg mice maintained on a high fat diet. However, plasma glucose levels during an intraperitoneal glucose tolerance test were higher in double Tg mice than in 3Tg mice (Fig. 7*A*). Insulin secretion during the intraperitoneal glucose tolerance test in double Tg mice was also lower than in 3Tg mice and was similar to WT littermates (Fig. 7*B*). Islet mass (β cell area) in double Tg mice was smaller than in 3Tg mice, again being similar to WT littermates (Fig. 7*C*). Furthermore, lipid peroxidation evaluated on the basis of the formation of TBARS was increased in plasma and WAT, but not in BAT or the liver, of double Tg mice compared with 3Tg mice (Fig. 7*D*). These data thus suggested that oxidative stress is reduced in WAT and plasma of aP2-KLF15 Tg mice as a consequence of the down-regulation of SCD1 expression in WAT, resulting in an increase in pancreatic β cell mass. The amounts of mRNAs for UCP2 and CPT1 in WAT of double Tg mice were reduced compared with 3Tg mice and were similar to WT littermates (Fig. 7*E*), suggesting that these changes might be related to the increase in the level of oxidative stress in WAT of double Tg mice compared with 3Tg mice.

DISCUSSION

Our previous observations suggested that KLF15 plays an essential role in adipogenesis in 3T3-L1 cells (5). However, it remained unclear whether KLF15 might play a similar role in adipose tissue *in vivo*. In this study, we first found that the expression of KLF15 is decreased in adipose tissue of obese mice. We then generated adipose tissue-specific KLF15 transgenic (aP2-KLF15 Tg) mice to investigate whether KLF15 contributes to various pathological conditions associated with obesity. These transgenic mice were found to manifest a complex phenotype characterized by increased insulin secretion from pancreatic β cells, leanness, and insulin resistance.

Our observation that the increased insulin secretion from pancreatic β cells in aP2-KLF15 Tg mice was normalized by the transgenic expression of SCD1 in WAT, with a concomitant increase in oxidative stress, suggested that the increased insulin

secretion in aP2-KLF15 Tg mice fed a high fat diet might be due to the reduced level of oxidative stress in these animals. Inhibition of SCD1 activity has previously been shown to lower oxidative stress (35, 36). We found that expression of the UCP2 gene was increased in WAT of aP2-KLF15 Tg mice compared with WT littermates. Furthermore, this increased expression of UCP2 in WAT and the reduced level of oxidative stress in aP2-KLF15 mice were abolished by WAT-specific expression of the SCD1 transgene. Given that UCP2 is the major uncoupling protein in WAT and that it reduces the mitochondrial production of ROS (35, 36), the increased expression of UCP2 in WAT of aP2-KLF15 Tg mice might contribute to the reduced level of oxidative stress in these animals. The increased insulin secretion from pancreatic β cells in aP2-KLF15 Tg mice was accompanied by an increase in β cell mass, with this latter effect also being eliminated in the double Tg mice. A similar increase in pancreatic β cell mass, accompanied by suppression of apoptosis without an effect on β cell proliferation, was previously shown to be induced in mice by antioxidant treatment (32). Pancreatic β cell failure, characterized by the inability of the cells to secrete sufficient amounts of insulin, is an important feature of type 2 diabetes. Oxidative stress is one of the many factors that have been found to contribute to β cell failure (30). Given that the major source of oxidative stress in the obese state is WAT (26), down-regulation of KLF15 expression in WAT of obese mice might be responsible, at least in part, for β cell failure as a result of the consequent up-regulation of SCD1 expression in WAT.

The aP2-KLF15 Tg mice manifested insulin resistance despite their resistance to diet-induced obesity. The reduced serum level of adiponectin in aP2-KLF15 Tg mice might be responsible for this insulin resistance. The serum adiponectin level is also decreased in mice lacking SCD1 specifically in adipose tissue as a result of gene deletion mediated by the Cre/loxP system (37). However, in this study, the serum adiponectin level was still decreased in double Tg mice, in which the expression of SCD1 in WAT is similar to that in WT littermates. Furthermore, the serum adiponectin level was decreased in aP2-KLF15 Tg mice fed a normal chow diet, even though there was no difference in the expression of SCD1 in WAT between aP2-KLF15 Tg and WT mice on this diet (data not shown). These observations thus suggest that the down-regulation of SCD1 expression in WAT is not responsible for the reduced serum level of adiponectin in aP2-KLF15 Tg mice. In addition, given that KLF15 did not inhibit the activity of the adiponectin gene promoter (data not shown), the reduced level of serum adiponectin in aP2-KLF15 Tg mice might be an indirect effect of KLF15 overexpression. Increased fat accumulation in the liver of KLF15 transgenics might also contribute to the hepatic insulin resistance as we observed increased TG levels concomitant with impaired insulin resistance in the liver of aP2-KLF15 Tg mice.

Increased O_2 consumption and resistance to diet-induced obesity were observed in aP2-KLF15 Tg mice and resistance to diet-induced obesity remained apparent in double Tg mice. Given that O_2 consumption was increased despite the reduced number of mitochondria in both BAT and WAT of aP2-KLF15 Tg mice, the up-regulation of proteins that contribute to mitochondrial function (such as CPT1) or to peroxisomal β-oxidation (such as acyl-CoA oxidase) in WAT or BAT might be responsible for these phenotypes.

Our *in vitro* analysis, including coculture experiments, supports that the metabolic phenotype seen in aP2-KLF15 transgenic mice is accounted for by the adipocytes, even if aP2 promoter-driven transgene expression was detected in both fat depots and macrophages (supplemental Fig. 1). However, we could not rule out the involvement of macrophage *in vivo*. It is a future direction to determine the relative contribution of macrophage using myeloid-specific KLF15 transgenic mice.

In summary, we have shown that overexpression of KLF15 in WAT and BAT resulted in increased insulin secretion from pancreatic β cells, the development of insulin resistance, and resistance to diet-induced obesity in mice. Furthermore, the down-regulation of SCD1 expression in WAT and the subsequent reduced level of oxidative stress appear to account for the increase in insulin secretion in aP2-KLF15 Tg mice. Our data thus provide an example of cross-talk between WAT and pancreatic β cells that is mediated through modulation of oxidative stress.

Acknowledgments—We thank B. M. Spiegelman and J. Miyazaki for plasmids, M. Saito for HB2 cells, and S. Seino for MIN6 cells.

REFERENCES

1. Kahn, B. B., and Flier, J. S. (2000) *J. Clin. Invest.* **106,** 473–481
2. Spiegelman, B. M., and Flier, J. S. (2001) *Cell* **104,** 531–543
3. Rosen, E. D., and Spiegelman, B. M. (2006) *Nature* **444,** 847–853
4. Uchida, S., Tanaka, Y., Ito, H., Saitoh-Ohara, F., Inazawa, J., Yokoyama, K. K., Sasaki, S., and Marumo, F. (2000) *Mol. Cell. Biol.* **20,** 7319–7331
5. Mori, T., Sakaue, H., Iguchi, H., Gomi, H., Okada, Y., Takashima, Y., Nakamura, K., Nakamura, T., Yamauchi, T., Kubota, N., Kadowaki, T., Matsuki, Y., Ogawa, W., Hiramatsu, R., and Kasuga, M. (2005) *J. Biol. Chem.* **280,** 12867–12875
6. Nagare, T., Sakaue, H., Takashima, M., Takahashi, K., Gomi, H., Matsuki, Y., Watanabe, E., Hiramatsu, R., Ogawa, W., and Kasuga, M. (2009) *Biochem. Biophys. Res. Commun.* **379,** 98–103
7. Gray, S., Feinberg, M. W., Hull, S., Kuo, C. T., Watanabe, M., Sen-Banerjee, S., DePina, A., Haspel, R., and Jain, M. K. (2002) *J. Biol. Chem.* **277,** 34322–34328
8. Yamamoto, J., Ikeda, Y., Iguchi, H., Fujino, T., Tanaka, T., Asaba, H., Iwasaki, S., Ioka, R. X., Kaneko, I. W., Magoori, K., Takahashi, S., Mori, T., Sakaue, H., Kodama, T., Yanagisawa, M., Yamamoto, T. T., Ito, S., and Sakai, J. (2004) *J. Biol. Chem.* **279,** 16954–16962
9. Teshigawara, K., Ogawa, W., Mori, T., Matsuki, Y., Watanabe, E., Hiramatsu, R., Inoue, H., Miyake, K., Sakaue, H., and Kasuga, M. (2005) *Biochem. Biophys. Res. Commun.* **327,** 920–926
10. Takashima, M., Ogawa, W., Hayashi, K., Inoue, H., Kinoshita, S., Okamoto, Y., Sakaue, H., Wataoka, Y., Emi, A., Senga, Y., Matsuki, Y., Watanabe, E., Hiramatsu, R., and Kasuga, M. (2010) *Diabetes* **59,** 1608–1615
11. Gray, S., Wang, B., Orihuela, Y., Hong, E. G., Fisch, S., Haldar, S., Cline, G. W., Kim, J. K., Peroni, O. D., Kahn, B. B., and Jain, M. K. (2007) *Cell Metab.* **5,** 305–312
12. Ntambi, J. M. (1999) *J. Lipid Res.* **40,** 1549–1558
13. Liu, X., Miyazaki, M., Flowers, M. T., Sampath, H., Zhao, M., Chu, K., Paton, C. M., Joo, D. S., and Ntambi, J. M. (2010) *Arterioscler. Thromb. Vasc. Biol.* **30,** 31–38
14. Cohen, P., Miyazaki, M., Socci, N. D., Hagge-Greenberg, A., Liedtke, W., Soukas, A. A., Sharma, R., Hudgins, L. C., Ntambi, J. M., and Friedman, J. M. (2002) *Science* **297,** 240–243
15. Jiang, G., Li, Z., Liu, F., Ellsworth, K., Dallas-Yang, Q., Wu, M., Ronan, J., Esau, C., Murphy, C., Szalkowski, D., Bergeron, R., Doebber, T., and

Zhang, B. B. (2005) *J. Clin. Invest.* **115,** 1030–1038
16. Gutiérrez-Juárez, R., Pocai, A., Mulas, C., Ono, H., Bhanot, S., Monia, B. P., and Rossetti, L. (2006) *J. Clin. Invest.* **116,** 1686–1695
17. Miyazaki, M., Flowers, M. T., Sampath, H., Chu, K., Otzelberger, C., Liu, X., and Ntambi, J. M. (2007) *Cell Metab.* **6,** 484–496
18. Matsushita, N., Kobayashi, K., Miyazaki, J., and Kobayashi, K. (2004) *J. Neurosci. Res.* **78,** 7–15
19. Sakai, T., Sakaue, H., Nakamura, T., Okada, M., Matsuki, Y., Watanabe, E., Hiramatsu, R., Nakayama, K., Nakayama, K. I., and Kasuga, M. (2007) *J. Biol. Chem.* **282,** 2038–2046
20. Miyake, K., Ogawa, W., Matsumoto, M., Nakamura, T., Sakaue, H., and Kasuga, M. (2002) *J. Clin. Invest.* **110,** 1483–1491
21. Seale, P., Conroe, H. M., Estall, J., Kajimura, S., Frontini, A., Ishibashi, J., Cohen, P., Cinti, S., and Spiegelman, B. M. (2011) *J. Clin. Invest.* **121,** 96–105
22. Nishino, N., Tamori, Y., Tateya, S., Kawaguchi, T., Shibakusa, T., Mizunoya, W., Inoue, K., Kitazawa, R., Kitazawa, S., Matsuki, Y., Hiramatsu, R., Masubuchi, S., Omachi, A., Kimura, K., Saito, M., Amo, T., Ohta, S., Yamaguchi, T., Osumi, T., Cheng, J., Fujimoto, T., Nakao, H., Nakao, K., Aiba, A., Okamura, H., Fushiki, T., and Kasuga, M. (2008) *J. Clin. Invest.* **118,** 2808–2821
23. Pagel-Langenickel, I., Schwartz, D. R., Arena, R. A., Minerbi, D. C., Johnson, D. T., Waclawiw, M. A., Cannon, R. O., 3rd, Balaban, R. S., Tripodi, D. J., and Sack, M. N. (2007) *Am. J. Physiol. Heart Circ. Physiol.* **293,** H2659–H2666
24. Li, F., Wang, Y., Zeller, K. I., Potter, J. J., Wonsey, D. R., O'Donnell, K. A., Kim, J. W., Yustein, J. T., Lee, L. A., and Dang, C. V. (2005) *Mol. Cell. Biol.* **25,** 6225–6234
25. Minami, K., Yano, H., Miki, T., Nagashima, K., Wang, C. Z., Tanaka, H., Miyazaki, J. I., and Seino, S. (2000) *Am. J. Physiol. Endocrinol. Metab.* **279,** E773–E781
26. Furukawa, S., Fujita, T., Shimabukuro, M., Iwaki, M., Yamada, Y., Nakajima, Y., Nakayama, O., Makishima, M., Matsuda, M., and Shimomura, I. (2004) *J. Clin. Invest.* **114,** 1752–1761
27. Laurent, G., Solari, F., Mateescu, B., Karaca, M., Castel, J., Bourachot, B., Magnan, C., Billaud, M., and Mechta-Grigoriou, F. (2008) *Cell Metab.* **7,** 113–124
28. Ikeda, K., Mutoh, M., Teraoka, N., Nakanishi, H., Wakabayashi, K., and Taguchi, R. (2011) *Cancer Sci.* **102,** 79–87
29. Hashimoto, N., Kido, Y., Uchida, T., Matsuda, T., Suzuki, K., Inoue, H., Matsumoto, M., Ogawa, W., Maeda, S., Fujihara, H., Ueta, Y., Uchiyama, Y., Akimoto, K., Ohno, S., Noda, T., and Kasuga, M. (2005) *J. Clin. Invest.* **115,** 138–145
30. Prentki, M., and Nolan, C. J. (2006) *J. Clin. Invest.* **116,** 1802–1812
31. Oliveira, H. R., Verlengia, R., Carvalho, C. R., Britto, L. R., Curi, R., and Carpinelli, A. R. (2003) *Diabetes* **52,** 1457–1463
32. Kaneto, H., Kajimoto, Y., Miyagawa, J., Matsuoka, T., Fujitani, Y., Umayahara, Y., Hanafusa, T., Matsuzawa, Y., Yamasaki, Y., and Hori, M. (1999) *Diabetes* **48,** 2398–2406
33. Tanaka, Y., Gleason, C. E., Tran, P. O., Harmon, J. S., and Robertson, R. P. (1999) *Proc. Natl. Acad. Sci. U.S.A.* **96,** 10857–10862
34. Oprescu, A. I., Bikopoulos, G., Naassan, A., Allister, E. M., Tang, C., Park, E., Uchino, H., Lewis, G. F., Fantus, I. G., Rozakis-Adcock, M., Wheeler, M. B., and Giacca, A. (2007) *Diabetes* **56,** 2927–2937
35. Diehl, A. M., and Hoek, J. B. (1999) *J. Bioenerg. Biomembr.* **31,** 493–506
36. Arsenijevic, D., Onuma, H., Pecqueur, C., Raimbault, S., Manning, B. S., Miroux, B., Couplan, E., Alves-Guerra, M. C., Goubern, M., Surwit, R., Bouillaud, F., Richard, D., Collins, S., and Ricquier, D. (2000) *Nat. Genet.* **26,** 435–439
37. Hyun, C. K., Kim, E. D., Flowers, M. T., Liu, X., Kim, E., Strable, M., and Ntambi, J. M. (2010) *Biochem. Biophys. Res. Commun.* **399,** 480–486